Can natural or anthropogenic explanations of late-Holocene CO$_2$ and CH$_4$ increases be falsified?

W.F. Ruddiman,[1] J.E. Kutzbach[2] and S.J. Vavrus[2]

Abstract

Concentrations of CO$_2$ and CH$_4$ in the atmosphere rose slowly during the millennia prior to the industrial era. Opposing explanations for these increases have invoked natural and anthropogenic sources. Here we revisit this argument using new evidence to see whether either explanation can be falsified (disproven, in the sense proposed by German philosopher Karl Popper). Two lines of evidence suggest that natural explanations for the CH$_4$ increase are falsified: (1) the absence of any sustained methane increase early in seven interglaciations prior to the Holocene; and (2) weakening emissions during the last 5000 years from the two largest global sources of CH$_4$ – north tropical and boreal wetlands. Consistent with this interpretation, a new synthesis of archeological data from southern Asia reported in this issue indicates an exponential increase in CH$_4$ emissions from expanding rice irrigation during the last 5000 years. Neither the anthropogenic nor the natural explanations for the CO$_2$ increase can at this point be falsified. Previous studies that rejected the early anthropogenic hypothesis based on the small size of early farming populations ignored a rich array of archeological and historical evidence showing that early farmers used much more land per capita than those in the centuries just before the industrial era. Previous interpretations of very small terrestrial (anthropogenic and other) carbon emissions during the last 7000 years based on the $\delta^{13}CO_2$ record failed to incorporate credible estimates of very large carbon burial in boreal peat lands during the late Holocene. Allowance for larger burial in peat deposits requires much greater emissions of anthropogenic carbon to balance the $\delta^{13}CO_2$ budget. The prevalence of downward CO$_2$ trends during equivalent intervals early in previous interglaciations poses a major problem for natural explanations of the late-Holocene CO$_2$ increase.

Introduction

Atmospheric concentrations of CO$_2$ and CH$_4$ increased during the last several thousand years. Ongoing arguments over whether these increases were natural or anthropogenic have focused mainly on two lines of evidence summarized in this paper. Part 1 examines gas trends from early in previous interglaciations. Rising concentrations like those in the Holocene would argue that the Holocene increases were natural, but falling trends in previous interglaciations would mark the Holocene increases as anomalous and thus anthropogenic. Part 2 explores changes in specific sources of CH$_4$ and CO$_2$ invoked in the natural and anthropogenic hypotheses. Part 3 assesses whether or not the evidence currently available is sufficient to falsify either the natural or anthropogenic explanations for the pre-industrial greenhouse-gas increases

Part 1. Holocene CO$_2$ and CH$_4$ trends versus prior interglaciations

Roughly every 100 000 years, Earth's climate emerges from a full glaciation into a full interglaciation with changes easily detected in climatic proxies from marine sediments and ice cores. Ice core records in Antarctica now extend to more than 800 000 years ago and penetrate previous interglaciations back to marine isotopic

stage 19. In this section, we compare Holocene greenhouse-gas trends against those in seven previous interglaciations: isotopic stages 5, 7, 9, 11, 15, 17, and 19. Isotopic stage 3, incorrectly identified as interglacial by Emiliani (1966), is omitted. Stage 13 is omitted because the deglaciation preceding it does not show a typically abrupt shift.

We use two methods to align Holocene gas concentrations against those in previous interglaciations. We call one method the 'insolation alignment' because it is based on orbital insolation. This method aligns the recent Northern Hemisphere summer insolation minimum at the precession period against the first comparable insolation minimum in each previous interglaciation. The timescales are shown as years before the precession insolation minima.

We call the other method the 'deglaciation alignment'. It aligns the beginning of the deglaciation that preceded the Holocene

[1]University of Virginia, USA
[2]University of Wisconsin-Madison, USA

Corresponding author:
W.F. Ruddiman, University of Virginia, Department of Environmental Sciences, Clark Hall, Charlottesville VA 22904 USA.
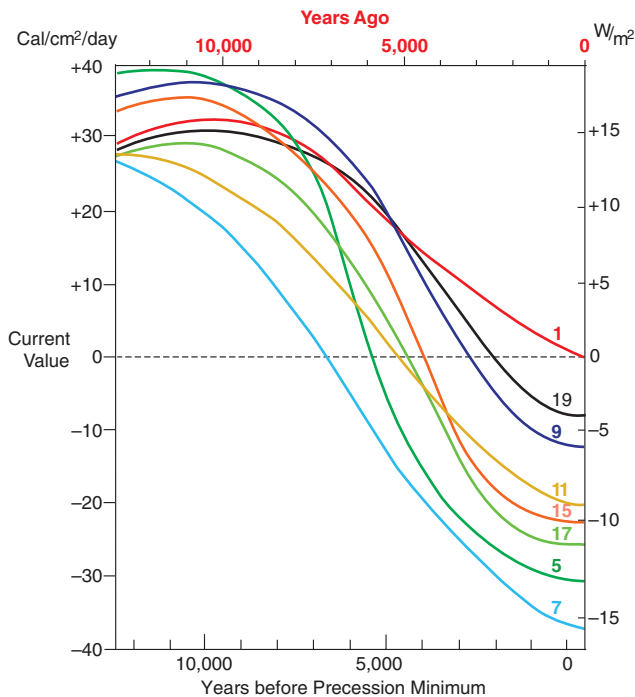Email: pisgahill@gmail.com

Figure 1. Caloric summer season insolation departures at 65°N from the present-day value for the Holocene (in red) and for equivalent intervals in previous interglaciations (numbered). All interglaciations are aligned on the first interglacial insolation minimum for the 21 June summer solstice at the precession cycle. From Berger (1978)

against the start of previous deglaciations defined by marine $\delta^{18}O$ trends. The timescale for the deglacial alignment comparison is shown as years subsequent to the beginning of each deglaciation.

The comparisons shown here use gas concentrations from Dome C, Antarctica (Loulergue et al., 2008; Lüthi et al., 2008; and prior studies referenced therein) plotted to the EDC3 time scale of Parrenin et al. (2007). The EDC3 timescale is based primarily on an ice-flow model, with a few tie-points linked to results from orbital tuning.

Insolation alignment

Because both tilt (obliquity) and eccentricity-modulated precession ($\epsilon\sin\omega$) play important roles in forcing various aspects of global climate, several insolation indices are available. The metric chosen here is the caloric summer insolation season devised by Milankovitch (1941) and compiled for 65°N latitude by Berger (1978). This metric calculates mean 65°N northern summer insolation for those 182 days of the year with higher values than the other 182 days. It expresses these variations as excesses or deficits relative to the modern value. This index gives greater emphasis to contributions from changes in tilt than do monthly mean calculations, which primarily reflect changes in eccentricity-modulated precession ($\epsilon\sin\omega$).

The current 65°N caloric summer-season insolation trend (Figure 1) is approaching a future minimum whose timing reflects two influences: a minimum in the contribution from the 22 000 year precession signal that was reached a few hundred years ago, and a minimum in the 41 000 year tilt signal that will occur roughly 10 000 years from now. The insolation alignments in

figure 1 for the 7 previous interglaciations are based on the Dome C timescale of Parrenin et al. (2007).

The corresponding alignments of the CH_4 and CO_2 trends for all eight interglaciations are shown in Figure 2. If we had chosen to align these signals on the precession insolation maximum near the end of each preceding deglaciation rather than on the first precession minimum within each interglaciation, the relative positions of the gas trends shown in Figure 2 would not have changed by more than 1000 years. In all cases, concentrations of both gases were lower during the late-deglacial intervals and then rose to peak concentrations early in each subsequent interglaciation, approximately 10 000 years before the present (or the earlier equivalents to the present).

In all eight interglaciations, the methane concentrations then fell toward lower values for several thousand years after the peak (Figure 2A). In the seven interglaciations prior to the Holocene, the CH_4 trends continued downward until the time equivalent to the present day, but the Holocene trend reversed direction 5000 years ago and gradually climbed back to the previous peak level. CH_4 concentrations in stage 19 show a brief upward excursion defined by two data points separated by ~1000 years, but then returned to lower values. Loulergue et al. (2008) interpreted this peak as a millennial-scale oscillation, and its brief duration differs from the longer-persisting methane rise of the last 5000 years. (The large negative CH_4 oscillation during the Younger Dryas near 12 000–11 000 years ago is another millennial-scale oscillation and will not be discussed further here.)

Most CO_2 trends followed a similar pattern (Figure 2B), with lower values during the late-deglacial intervals, increases to peak CO_2 concentrations early in the following interglaciation, and then decreases toward the present. Once again, the CO_2 trend in the late Holocene differs from the others: it rose by ~22 ppm, while six of the seven other trends fell, some by small amounts (stages 5 and 11), and others by larger amounts (stages 7, 9, and 19). One previous interglaciation (isotopic stage 15, discussed later) shows a slow CO_2 increase of ~ 8 ppm (Figure 2B).

In summary, not one of the seven previous interglaciations shows an upward CH_4 trend like that in the late Holocene, and only one shows an upward CO_2 trend (Table 1). Given the impossibility of significant anthropogenic influences in earlier interglaciations, these downward gas trends must have been natural in origin.

Deglaciation alignment. EPICA (2004) and Broecker and Stocker (2006) used a different method to align Holocene gas trends against those in interglacial stage 11. They aligned the beginning of the two preceding deglaciations and counted forward in 'time elapsed' since the start of the deglaciations. Here we apply their method to all seven previous interglaciations. Because marine benthic foraminiferal $\delta^{18}O$ records are the most common measure of global ice volume (and thus deglacial ice melting), we use the multicore global $\delta^{18}O$ stack of Lisiecki and Raymo (2005) for this alignment.

The initial $\delta^{18}O$ decreases that define the start of the deglaciations (Figure 3) began abruptly and can be defined with little uncertainty. The estimated ages of these first decreases in the marine $\delta^{18}O$ stack agree to within about 1000 years with the estimated ages of the first shifts in the δD index of air temperature over Antarctica to more positive (warmer) values based on the
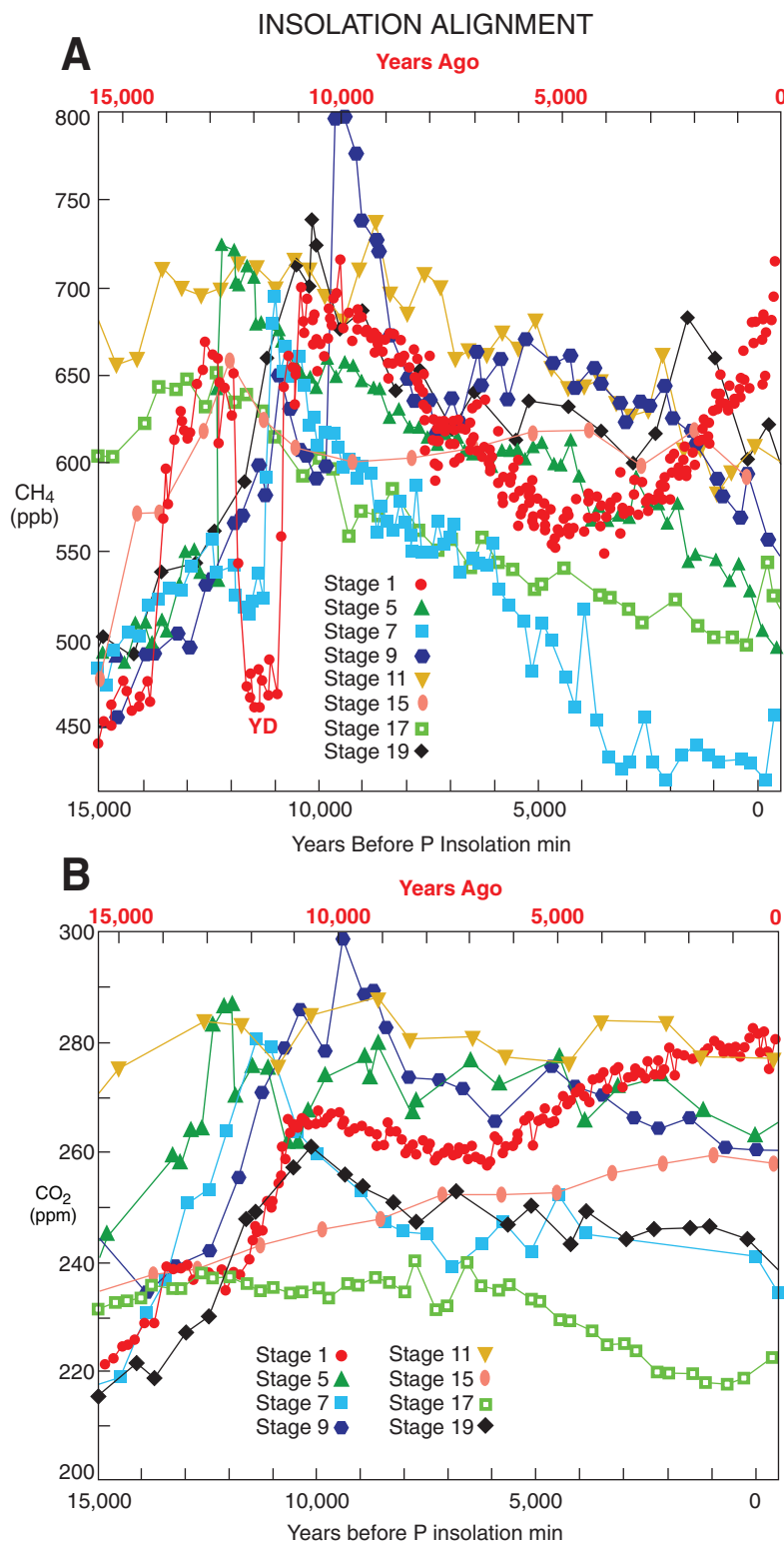
INSOLATION ALIGNMENT

A

B

Figure 2. Dome C concentrations of (A) CH_4 and (B) CO_2 for the Holocene and seven previous interglaciations using the insolation alignments shown in Figure 1 and Dome C age estimates from the EDC gas timescale (Parrenin et al., 2007). Gas concentrations from Lüthi et al. (2009); Loulergue et al. (2008); and references therein

EDC3 timescale (Jouzel et al., 2007). Using Dome C δD trends to define the deglacial onsets instead of $\delta^{18}O$ would have given almost exactly the same alignments as those shown in Figure 3.

Picking the ends of the deglaciations is more difficult. The $\delta^{18}O$ trends end in 'tails' that gradually approach full-interglacial values, with sample-to-sample $\delta^{18}O$ variations often falling within the analytical error of the $\delta^{18}O$ method. To minimize uncertainty

in choosing the end of the deglaciations, we truncated each deglacial 'tail' at the level where the decreasing $\delta^{18}O$ values first attained 90% of the net $\delta^{18}O$ change across that deglaciation.

Two groups of deglaciations are evident in Figure 3. The five deglaciations that preceded stages 1, 5, 7, 9, and 19 were short, lasting ~10 000 ± 1000 years. The other three were longer: ~14 000 years for the deglaciation preceding stage 15, ~18 000

Table 1. CO_2 and CH_4 trends during previous interglaciations based on insolation alignment

Natural explanations predict **CH_4 and CO_2 increases like those in the Holocene**
Anthropogenic explanation predicts **CH_4 and CO_2 decreases unlike the Holocene increases**

Interglaciation	CH_4 trend	CO_2 trend
Stage 5	**decrease**	**decrease**
Stage 7	**decrease**	**decrease**
Stage 9	**decrease**	**decrease**
Stage 11	**decrease**	**[decrease]**
Stage 15	**decrease**	i**ncrease***
Stage 17	**decrease**	**decrease**
Stage 19	**decrease**	**decrease**

[] Small trend.
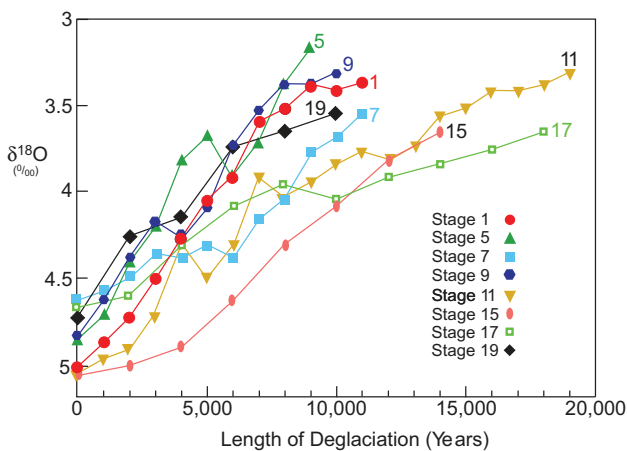* No-analog $\delta^{18}O$ (ice-volume) trend.

Figure 3. Trends in $\delta^{18}O$ from the deglaciations preceding the Holocene and seven previous interglaciations, from Lisiecki and Raymo (2005). The trends are truncated where they reach 90% of the total amplitude of $\delta^{18}O$ change across each deglaciation

years for the one before stage 17, and ~19 000 years for the one prior to stage 11.

The gas concentration trends produced by this alignment method vary widely during the times equivalent to the late Holocene CH_4 and CO_2 rises (Figure 4). For CH_4, stages 5, 7, 9, 17, and 19 show downward trends during the intervals comparable to the late Holocene. The stage 15 trend is level. Stage 11 initially has a downward trend, followed by a sharp upturn, and a small final drop. For CO_2, the four interglaciations that were preceded by short deglaciations (stages 5, 7, 9, and 19) all show downward trends; two interglaciations (stages 11 and 17) have relatively stable trends; and one (stage 15) has an upward trend.

In summary, of seven previous interglaciations tested with the deglaciation alignment, a majority of the cases show downward CH_4 and CO_2 trends, and only one shows an upward CH_4 or CO_2 trend (Table 2). The prevalence of downward or level gas trends again suggests that the marked upward trends during the late Holocene were departures from normal, and not of natural origin.

Evaluation of the alignment methods. <u>Insolation alignments.</u> The CH_4 and CO_2 trends for the insolation alignment in Figure 2 are based on a timescale (EDC3) that does not result from 'tuning' ice-core proxies to assumed orbital drivers. As a result, these trends avoid the circular reasoning that would arise in assessing results from an astronomically tuned timescale. The question at

hand is whether aligning the EDC3 ages to the astronomically dated orbital trends in Figure 1 is a meaningful exercise.

Several observations justify the claim that methane changes are predictably aligned to insolation. The orbital monsoon theory of Kutzbach (1981) predicts that low-latitude insolation (primarily at the 22 000 year precession cycle) drives changes in monsoon intensity across a broad span of the northern continents from North Africa through Arabia and India and eastward to China. COHMAP (1988) found that this relationship explains the gradual drying of northern wetlands, which were a major source of methane during the early Holocene. Speleothem $\delta^{18}O$ data summarized by Burns (2011, this issue) confirm this pervasive drying trend. Over longer timescales, the remarkably coherent relationship between cave-calcite $\delta^{18}O$ values in China and low-latitude insolation provides unequivocal confirmation of this monsoonal forcing-and-response relationship (Wang et al., 2007). Based on a wide range of evidence, methane releases from north-tropical wetlands have long been regarded as the largest factor in ice-core CH_4 variations (Brook et al., 2000; Chappellaz et al., 1997).

For the Holocene, this link is further supported by the close alignment of the CH_4 maximum in GRIP ice dated by annual layering (Blunier et al., 1995) with the most recent 65°N caloric summer-season insolation maximum 11 000–10 500 years ago (Figures 1, 2). In addition, a timescale for Vostok ice based on tuning methane variations to the 22 000 year northern insolation cycle spanning the last 300 000 years (Ruddiman and Raymo, 2003) resembles two other Vostok timescales based on entirely different methods (Ruddiman, 2007). This wide range of evidence justifies using the 'insolation alignment' method to evaluate the methane variations.

The relationship of CO_2 changes to insolation is more complex. CO_2 is highly correlated to the $\delta^{18}O$ index of ice volume (and deep-ocean temperature) during the last 800 000 years because carbon moves from the atmosphere into the deep ocean during glaciations and comes back out during interglaciations. But the mechanisms controlling this transfer and the link or links to insolation remain unclear. Nevertheless, the strong connection between methane variations and 65°N caloric summer-season insolation is by itself sufficient to show that insolation is a valid basis for aligning the entire gas phase in Dome C ice (both CH_4 and CO_2).

The one exception to the downward CO_2 trends during previous interglaciations is the slow CO_2 rise during stage 15 (Figure 2). But stage 15 is also unique in another respect: the $\delta^{18}O$ signal continued to decrease throughout that entire early-interglacial interval rather than leveling out at peak-interglacial values. This ongoing $\delta^{18}O$ decrease through the first 10 000 years of the stage 15 'interglaciation' suggests that residual ice sheets were still slowly melting (for reasons that remain unclear), rather than stabilizing or beginning to regrow as in the other interglaciations. Given the close correlation between CO_2 and $\delta^{18}O$ during the last 800 000 years, it seems likely that this anomalous CO_2 increase in stage 15 is tied to the anomalous $\delta^{18}O$/ice trend. The continuing ice melting early in stage 15 makes it a poor analog for the last 7000 years of the Holocene, when ice volume had reached a stable minimum.

In summary, both theory and wide-ranging observations demonstrate a strong link between methane changes and 65°N caloric summer-season insolation. This link validates the insolation alignment of gas trends shown in Figure 2.

<u>Aligning on deglaciations.</u> Aligning previous interglaciations on the onset of the prior deglaciations and counting forward in
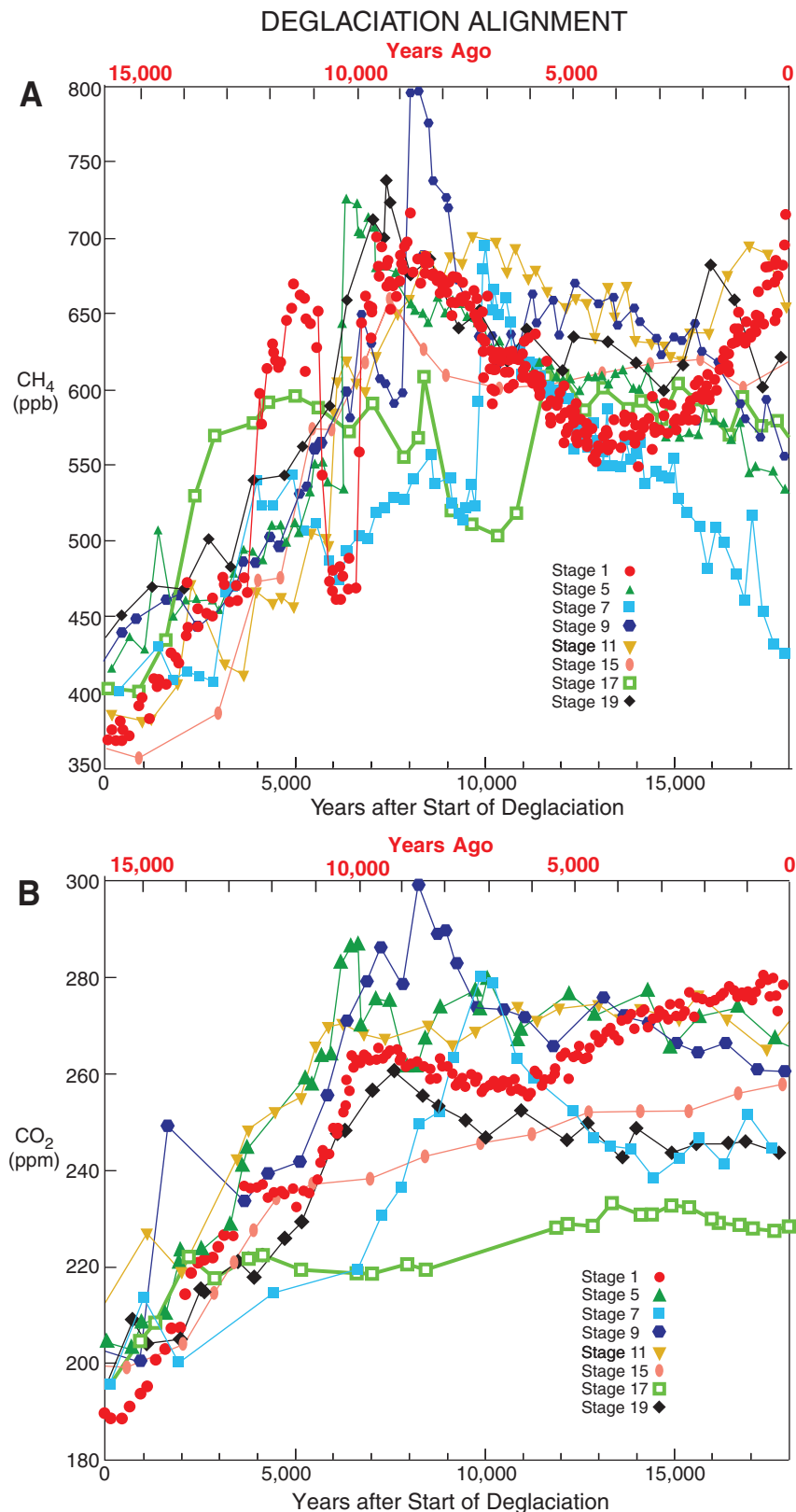
DEGLACIATION ALIGNMENT

Figure 4. Dome C concentrations of (A) CH$_4$ and (B) CO$_2$ for the Holocene and seven previous interglaciations using the deglacial δ^{18}O alignments in Figure 3 and Dome C age estimates from the EDC gas timescale (Parrenin et al., 2007). Gas concentrations from Lüthi et al. (2009); Loulergue et al. (2008); and references therein

time carries the implicit assumption that all deglaciations developed in similar ways. Yet Figure 3 shows that deglaciations defined by δ^{18}O trends varied in length from ~10 000 years to almost 20 000 years. This wide range raises the question of whether the varying durations of these deglaciations affected the relative alignments of the subsequent interglaciations.

Stage 11 has often been used as a possible analog to stage 1 because eccentricity-modulated precession ($\varepsilon\sin\omega$) values were low in amplitude at both times. EPICA (2004) and Broecker and Stocker (2006) aligned the two interglaciations based on the time elapsed since the onset of the previous deglaciations, but the δ^{18}O decreases in Figure 3 show that the

Table 2. CO_2 and CH_4 trends during previous interglaciations based on deglaciationalignment

Natural explanations predict **CH_4 and CO_2 increases like those in the Holocene**

Anthropogenic explanation predicts **CH_4 and CO_2 decreases unlike the Holocene increases**

Interglaciation	CH_4 trend	CO_2 trend
Stage 5	decrease	decrease
Stage 7	decrease	decrease
Stage 9	decrease	decrease
Stage 11	decr/incr	----
Stage 15	----	increase*
Stage 17	decrease	----
Stage 19	decrease	decrease

* No-analog $\delta^{18}O$ (ice-volume) trend.
Dashed lines indicate no clear trend.

stage 12/11 deglaciation lasted almost twice as long as the stage 2/1 transition.

Rohling et al. (2010) found that the deglacial alignment method produced a complete misalignment of the full stage 11 and stage 1 interglaciations because of the differing lengths of the two preceding deglaciations. Based on sea-level evidence from the Red Sea, they confirmed a conclusion previously suggested by the marine global $\delta^{18}O$ stack of Lisiecki and Raymo (2005) and evident in Figure 5A. If the deglacial alignment method is used, the full interglaciations in stages 11 and stage 1 do not overlap in time at all. The entire stage 1 interglaciation correlates with the latter part of the stage 12/11 deglaciation, and the stage 11 interglaciation doesn't begin until a time equivalent to several thousand years from now. Thus the deglacial-onset method fails to align the Holocene with stage 11. Crucifix and Berger (2006) and Ruddiman (2006) have also criticized the alignments proposed by Broecker and Stocker (2006) for similar reasons.

The evidence from Rohling et al. also overturns another misconception about stage 11. The long interval of near-interglacial warmth registered by indicators such as Antarctic ice-core δD values has been interpreted as indicating a 'long interglaciation' that would imply a much longer future duration for the current interglaciation. However, much of the interval of positive δD values shown in Figure 5B falls on the latter part of the stage 12/11 deglaciation. At this time, the δD values had not yet reached full-interglacial levels. The warmest full-interglacial temperatures (heaviest δD values) were constrained to the full stage 11 interglaciation and lasted for less than 10 000 years. These results invalidate the argument of EPICA (2004) and Broecker and Stocker (2006) that the current interglacial still has some 16 000 years left to run. They also disagree with the conclusion of Berger and Loutre (2003) that the current interglaciation has another 50 000 years left to run. Instead, the falling δD values just after the full stage 11 interglaciation in Figure 5B indicate that the current Antarctic warmth defined by δD values should have ended by now.

Of the seven previous interglaciations aligned on deglacial onsets in Figure 3, four were preceded by deglaciations that lasted for roughly the same 10 000 years as the deglaciation prior to the Holocene. In all of these cases, the alignments of the subsequent interglaciations with the late Holocene are very similar to those produced by the insolation alignment method – all four show downward CO_2 and CH_4 trends (Figure 4).

In summary, on close inspection, the one past interglaciation for which the deglacial-alignment method has been proposed fails
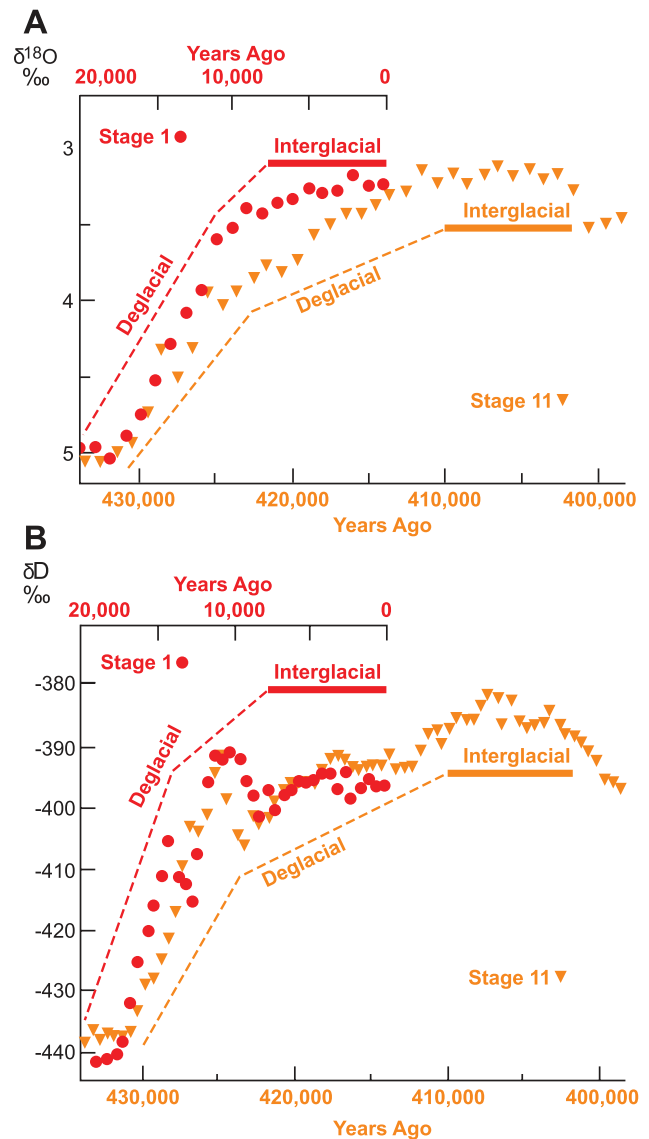

Figure 5. (A) Benthic $\delta^{18}O$ data for marine isotopic stages 12 to 11 and 2 to 1 from Lisiecki and Raymo (2005) plotted by aligning the onsets of the two deglaciations. Dashed lines indicate intervals of deglaciation. Solid red and orange bars show intervals when global sea level was at full interglacial values. (B) Dome C δD trends from Jouzel et al. (2007) plotted as in Figure 5A. including deglaciations and full interglaciations

its own test because of the differing lengths of the preceding deglaciations. Moreover, a majority of the comparisons based on the deglacial-alignment method shows downward gas trends like those from the insolation alignments.

Based on the strong justification for the insolation alignment method, the Holocene CH_4 and CO_2 trends at Dome C are compared with a stacked average of the trends from six previous interglaciations in Figure 6. The stage 15 interglaciation was omitted because of the no-analog ice-volume boundary condition. Gas measurements from each previous interglaciation were binned into 1000-year intervals and averaged. For a few intervals in previous interglaciations with no measurements, values were calculated by averaging those in the prior and subsequent bins.

The CH_4 and CO_2 trends in the early part of the Holocene fall close to the stacked average from the previous interglaciations and well within the standard deviations (Figure 6). After 7000 years ago, the Holocene CO_2 trend began to trend upward while
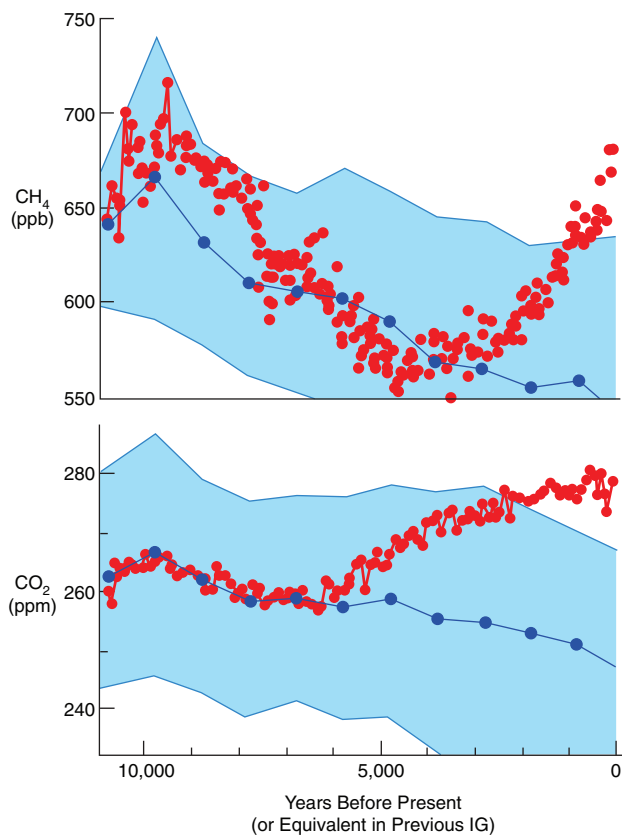
Figure 6. Comparison of Dome C Holocene trends of (A) CH$_4$ and (B) CO$_2$ (red circles) with values calculated by averaging similar portions of six previous interglaciations (blue circles). Light blue shading shows one standard deviation around the previous-interglacial means

the average from the six previous interglaciations continued to fall. By 2000 years ago, the CO$_2$ concentration had moved outside the one standard deviation envelope. Starting 5000 years ago, the Holocene CH$_4$ trend also began to rise while the prior-interglacial average continued to fall, and by 1000 years ago it had emerged above the one standard deviation envelope. This comparison further suggests that the Holocene CO$_2$ and CH$_4$ increases in recent millennia were not natural.

Part 2. Late-Holocene greenhouse-gas sources

A second way to evaluate natural and anthropogenic causes of the late-Holocene greenhouse-gas increases is to examine the proposed sources. Changes in the anthropogenic sources need to explain not just the late-Holocene gas increases but the additional departures from the downward trends early in previous interglaciations (Figure 6).

Sources of methane

Natural CH$_4$ sources. Wetlands are the major natural source of methane. Three wetland regions are large enough to be potential explanations for the late-Holocene CH$_4$ increase (Table 3A).

Wetlands in boreal regions of Eurasia and North America can be ruled out as the source because the difference in CH$_4$ concentration between Greenland and Antarctic ice has been decreasing for almost 5000 years. This decreasing trend indicates reduced

Table 3. Natural and anthropogenic sources of late-Holocene CH$_4$

	Change during late Holocene	Evidence
A. Natural sources		
Boreal wetlands (−58‰)	**Decreasing**	Greenland/Antarctic CH$_4$ gradient
N Tropical/subtropical wetlands (−58‰)	**Decreasing**	Lake levels, pollen, cave calcite $\delta^{18}O$
S Tropical/subtropical wetlands (−58‰)	**Increasing**	Lake levels, pollen, cave calcite $\delta^{18}O$
Global natural burning (−25‰)	Unknown	Charcoal, pollen
B. Anthropogenic sources		
Domesticated livestock (−60‰)	**Increasing**	Archeology, history
Rice irrigation (−63‰)	**Increasing**	Archeology, history
Biomass burning (−25‰)	**Increasing**	Archeology, history
Human waste (−60‰)	**Increasing**	Archeology, history

CH$_4$ fluxes to Greenland ice from nearby boreal sources, and greater fluxes from low-latitude (tropical or near-tropical) sources lying more nearly equidistant between the two ice sheets. Although Schmidt et al. (2004) inferred increasing late-Holocene boreal fluxes based on the methane gradient, Chappellaz et al. (1997) had actually found a large decrease between an interval centered on ~3750 years ago and one centered on ~650 years ago. A subsequent high-resolution comparison by Brook and Mitchell (2007) further confirmed that the interhemispheric CH$_4$ gradient has been decreasing since 4700 years ago. The extent of boreal peat lands increased during the last 5000 years (Gorham, 1991; Yu, 2011, this issue; Yu et al., 2009), but summers were cooling (Foley et al., 1994). The cooler boreal summers apparently suppressed late-Holocene methane releases.

Natural wetlands in the northern tropics and subtropics can also be ruled out as the CH$_4$ source because northern monsoon rains were weakening (Kutzbach, 1981). COHMAP (1988) compiled evidence of lower lake levels and increases in pollen from dry-adapted vegetation across a broad swath from North Africa to India and southern China. Cave calcite sequences in China and Oman (summarized by Burns, 2011, this issue) show large $\delta^{18}O$ increases that can only be explained by progressive monsoon weakening. Both lines of evidence indicate reduced methane emissions across a vast area of the northern tropics and extra-tropics during the Holocene.

The only extensive wetland region left is the Amazon Basin, much of which lies south of the equator. Summer insolation drives monsoon circulations in the Southern Hemisphere with a timing exactly opposite that in the north. During Southern Hemisphere summer (December–February), insolation increased during the late Holocene and drove a strengthening monsoon with greater precipitation in the Southern Amazon Basin. Evidence of increased monsoonal moisture in this region includes $\delta^{18}O$ trends in cave calcite from southeastern Brazil (Cruz et al., 2005; Burns, 2011, this issue) and rising lake levels in the Andes on the western edge of the South American summer monsoon region (Selzer et al., 2000).
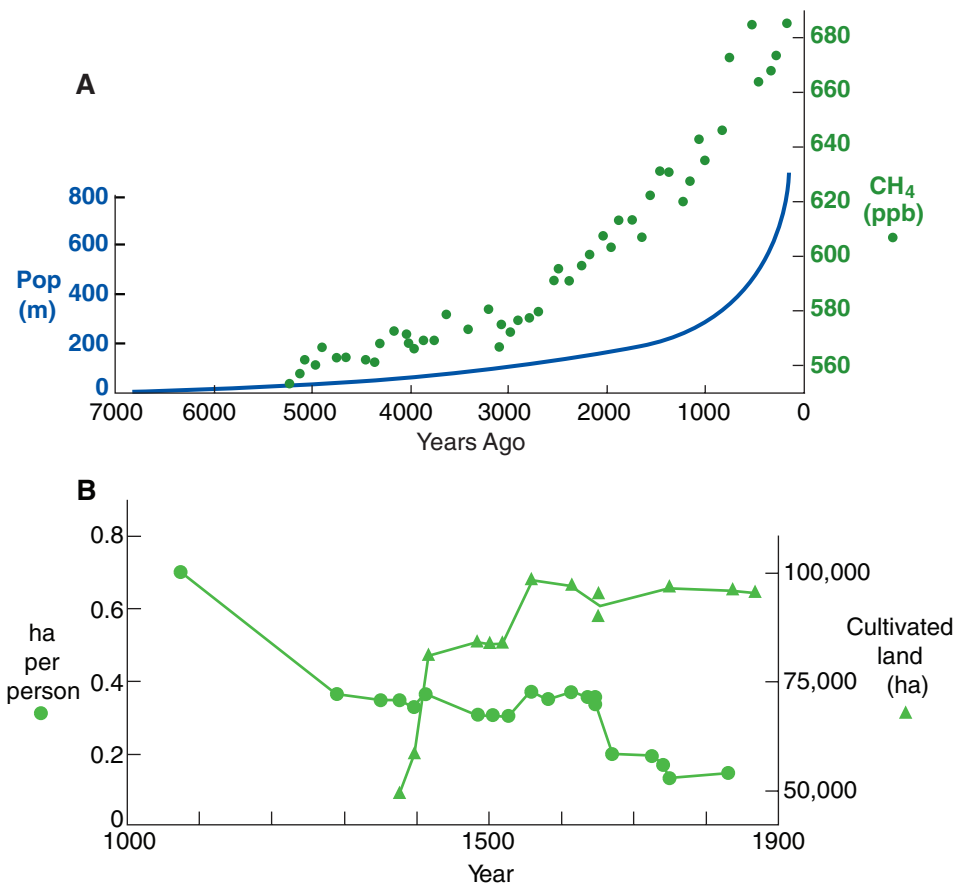
Figure 7. (A) Comparison of late Holocene CH₄ trend at Dome C (Lourlergue et al., 2009) with estimated global population (from Ruddiman and Ellis, 2009; based on Denevan, 1992 and McEvedy and Jones, 1978). (B) Changes in per-capita and total crop land in the Lake Tai region of the lower Yangtze River valley, China during the late historical interval (Ellis and Wang, 1997)

Despite this increase in regional methane release, several lines of evidence indicate that southern Amazonian sources are unlikely to have taken control of global fluxes 5000 years ago and caused the CH₄ increase. Previous interglaciations (Figure 2A) all show downward CH₄ trends during times equivalent to the late Holocene, and these decreases fit the pattern expected from control of methane concentrations by north-tropical and boreal monsoonal sources (as inferred by Brook, et al., 2000 and Chappellaz et al., 1997). Although southern methane sources almost certainly were increasing early in previous interglaciations, northern sources overwhelmed the Amazon sources in the global-average trend.

In addition, simulations of longer orbital timescales with models indicate a dominant Northern Hemisphere methane source. In the FOAM model, monsoon variations in South America were only about half the amplitude of those in southeast Asia and North Africa (Kutzbach et al., 2007). Also, Brovkin et al. (2002) simulated a major Holocene weakening of monsoon precipitation across a large geographic area in the north, compared with a much weaker monsoonal increase in a smaller region of South America. This difference in monsoon responses is expected because of the larger land masses in the Northern Hemisphere and the elevated Tibetan Plateau.

These lines of evidence argue against the possibility that South American sources could have taken control of the global methane trend 5000 years ago. Other considerations also point to a dominant Northern Hemisphere source. The part of the Amazon Basin lying north of the equator follows the Northern Hemisphere pattern, rather than the Southern. And neither southern Africa nor Australia has extensive wetland sources of methane.

Methane is also released when grasslands burn through natural causes (Table 3A). Charcoal accumulation rates are a potential index of changes in natural rates of burning, but the patterns have been regionally heterogeneous during the late Holocene. In several regions where slow increases in charcoal burial have occurred, deforestation by humans is considered a likely complicating factor (Carcaillet et al., 2002).

Anthropogenic CH₄ sources. Several anthropogenic activities have been sources of increasing pre-industrial methane emissions: rice irrigation, livestock tending, biomass burning, and a small input from human waste (Table 3B). As agriculture spread across every continent except Australia and Antarctica during the last 5000 years, emissions from all of these sources grew (Ruddiman, 2003; Ruddiman et al., 2008).

Although both global population and methane concentrations rose rapidly during the late Holocene, much of the CH₄ rise occurred prior to 1000 years ago, whereas most of the exponential population increase occurred after that time (Figure 7A). If human activities are to be invoked as the cause of the methane increase, there must have been some decoupling between the two signals such that earlier populations produced larger per-capita emissions than later ones (Ruddiman and Thomson, 2001).

In the case of rice irrigation, long historical records compiled by Ellis and Wang (1997) from a rice-growing region (Wuxi County) in the lower Yangtze River area show evidence of such a decoupling (Figure 7B). Although the regional population increased by a factor of almost 40 between AD 300 and 1750, the total area under

cultivation leveled out by 1600 because every available piece of arable land (90% of the countryside) was under cultivation by that time. The small increase in cropland between 1500 and 1550 reflects conversion of low-lying brackish areas and other similarly marginal acreage to rice agriculture (Ellis and Wang, 1997).

With population rising but with little increase in total area cultivated, per-capita land use for farming fell from ~0.7 ha in 1100 to ~0.15–0.2 ha in the 1700s and early 1800s (Figure 7B). This trend toward 'intensification' (obtaining more food per area farmed) resulted from several factors: increased use of organic fertilizer (vegetable debris, livestock manure, ash, and 'night soil'), more intense labor (eliminating pests and weeds by hand), and planting multiple crops per year (one or two rice crops in the warm season and a dry land crop in the cold season). If extrapolated to other regions across Southeast Asia, this decreasing per-capita trend could reconcile the seeming mismatch in Figure 7A between the rises in methane emissions and in population.

Additional evidence reconciling this timing mismatch comes from a new archeological summary by Fuller et al. (2011, this issue), who inferred that the area of Asia devoted to rice farming increased exponentially between 5000 and 1000 years ago, reaching ~35% of modern values, even though the population had only reached ~6% of the modern level by 1000 years ago. By their estimate, methane emissions from rice irrigation were sufficient to account for most of the CH_4 increase in ice cores between 5000 and 1000 years ago.

Fuller et al. (2011, this issue) also mapped the spread of livestock across Asia and Africa in the middle and late Holocene. They inferred that methane emissions from livestock would also have had a large effect on CH_4 emissions between 5000 and 1000 years ago but did not attempt a quantitative estimate. The numerical ratio of humans and livestock would also have changed over time. Ellis and Wang (1997) noted that farmers were gradually forced to reduce their per-capita livestock holdings during the later historical era because the rapidly increasing population density drove a need for more nutrition and because pasture and livestock produced less nutrition per hectare than intensive crop farming. As a result, methane emissions from livestock on a per-capita (human) basis also fell in the late historical era.

Finally, Ferretti et al. (2005) found isotopic evidence that early Americans had been doing an unexpectedly large amount of biomass burning prior to being decimated by European diseases in the 1500s (see also Mischler et al., 2009). Elimination of most of the early American population reduced the global per-capita amount of biomass burning after 1500.

In summary, archeological data show that early agriculture is a promising explanation for the late-Holocene methane anomaly. Higher per-capita CH_4 emissions by early farmers can reconcile the somewhat earlier rise in methane concentrations compared to the population trend.

The carbon isotopic composition of atmospheric methane ($\delta^{13}CH_4$) also has the potential to help distinguish among possible sources of methane (Table 3). As the atmospheric CH_4 concentration rose in the late Holocene, the $\delta^{13}CH_4$ value varied between −47 and −49‰ (Ferretti et al., 2005; Mischler et al., 2009).

Natural explanations would require a near-balance between increased delivery of highly negative carbon (−58‰) from natural wetlands and more positive carbon (−25‰) from grasslands. The two increases would have to have been in the ratio ~30/70 to keep the atmospheric $\delta^{13}CH_4$ value close to the −48‰ mean, but this explanation runs into the constraints discussed earlier. The extensive drying of northern monsoonal regions and cooling of

Table 4. Natural and anthropogenic sources of late-Holocene CO_2

	Change during late Holocene	Evidence
A. Natural sources		
Ocean $CaCO_3$ chemistry (−6‰)	**Increasing?**	Marine sediments
Coral reefs (−6‰)	**Increasing?**	Marine geology
Ocean temperature/solubility (−6‰)	**Increasing**	Benthic marine $\delta^{18}O$
Natural terrestrial C releases (−25‰)	**Increasing**	Lake-sediment pollen and biome modeling
Natural boreal C storage (+25‰)	**Increasing (storage)**	Peat cores
B. Anthropogenic sources		
Deforestation (−25‰)	**Increasing**	Archeology, history
Coal and peat burning (−25‰)	**Increasing**	History
Ocean temp/solubility feedback (−6‰)	**Increasing**	Benthic marine $\delta^{18}O$
Southern Ocean feedback (−6‰)	**Increasing?** (Not decreasing)	Ice-core δD

boreal regions were reducing (rather than enhancing) emissions of −58‰ methane, and the increasing CH_4 input from southern Amazonia seems very unlikely to have compensated for this large decrease in the north. Charcoal data show somewhat heterogeneous regional burning trends, with likely human overprints.

The anthropogenic explanation for the nearly constant $\delta^{13}CH_4$ value requires a similarly proportioned balancing between increases in negative carbon from rice paddies (−63‰) and livestock (−60‰) against increases of more positive carbon from anthropogenic burning of grass (−25‰). Because all of these anthropogenic CH_4 sources were increasing, this explanation remains viable, but further work is needed to quantify the relative emissions.

Sources of CO_2

Natural CO_2 sources. Several natural explanations have been proposed to explain the CO_2 rise during the last 7000 years (Table 4).

Broecker et al. (1999) proposed an ocean carbonate compensation mechanism triggered by late-deglacial advance of forests into regions from which the melting ice sheets had retreated. As northern forests grew, they extracted hundreds of billions of tons of carbon from the ocean. This transfer threw ocean chemistry out of balance by reducing CO_2-related acidity and permitting deposition of extra $CaCO_3$ on the seafloor. When high-latitude forests stopped advancing and sequestering oceanic carbon near 7000 years ago, ocean carbonate chemistry adjusted toward a new equilibrium. Increased acidity dissolved $CaCO_3$ on the seafloor, which added carbonate ions (CO_3^{-2}) to seawater and emitted hundreds of billions of tons of CO_2 to the atmosphere.

Modelers have simulated this mechanism by parameterizing numerical (impulse) responses to an assumed imbalance in carbonate chemistry that reflects the initial deglacial carbon transfer from the ocean to the land. Estimates of the size of this transfer generally range between 300 and 700 GtC (Bird et al., 1996), although large amounts of carbon may have been stored in permafrost regions during glacial times and released during deglacial warming (Zimov et al., 2009). In the latter case, the net deglacial carbon transfer to the land would have been smaller, as would the subsequent rise in atmospheric CO_2 from the ocean chemistry mechanism.

The carbonate compensation hypothesis continues to remain vulnerable to a criticism originally raised by Ruddiman (2003). Because forests advanced northward into regions where ice sheets were melting during all of the previous deglaciations, the hypothesis predicts past CO_2 rises like the one that occurred in the Holocene. As shown in Figure 2, however, none of the previous interglaciations shows rising CO_2 values during times equivalent to the late Holocene, except for the slow increase during the no-analog stage 15.

The coral-reef hypothesis (Ridgwell et al., 2003) proposes that reef construction accelerated after the ocean stabilized at or near peak-interglacial sea levels near 7000 years ago. Building reefs made of $CaCO_3$ and $MgCO_3$ extracted carbonate ions from the ocean, which was left richer in CO_2 and thus transferred more CO_2 to the atmosphere. Ridgwell et al. (2003) estimated that reef formation could have driven atmospheric CO_2 concentrations higher by 40 ppm, compared with the ~22 ppm increase actually observed.

Field data are not sufficient to provide accurate constraints on Holocene rates of reef construction on a globally integrated basis, although Vecsei and Berger (2004) estimated that this mechanism could have released ~110 GtC after 6000 years ago, enough to drive CO_2 concentrations higher by ~ 8 ppm. Again, however, the coral-reef hypothesis faces the problem of explaining the contradictory downward CO_2 trends during previous interglaciations (Figure 2B). The problem is most acute during interglacial stage 11, when sea level remained at peak-interglacial values from ~410 000 to ~402 000 years ago (Figure 5A), yet CO_2 concentrations did not increase.

An early study by Indermuhle et al. (1999) suggested that natural releases of terrestrial carbon could have played a major role in the CO_2 rise, but later work by the Bern group concluded that those releases accounted for no more than a few ppm of the observed increase (Joos et al., 2004). Another potential factor, global sea-surface temperature changes during the Holocene, has generally been regarded as secondary because the change is uncertain in sign and small in amplitude. In the view of the Bern group (Elsig et al., 2009), most of the observed CO_2 rise since 7000 years ago is explained by carbonate compensation and coral reef construction.

Anthropogenic CO_2 sources. In the early anthropogenic hypothesis, Ruddiman (2003) proposed that deforestation can explain the 22 ppm Holocene CO_2 rise and might also account for a total Holocene CO_2 anomaly of ~40 ppm. Joos et al. (2004), however, estimated an anthropogenic effect of just a few ppm based on two arguments: simulations from land-use models showing minimal pre-industrial forest clearance, and constraints from $\delta^{13}CO_2$ measurements.

Criticisms based on land-use simulations implicitly or explicitly take note of the mismatch between the substantial CO_2 increase several millennia ago compared with the still-small global population at that time (Figure 8A). Most modeling studies have assumed that per-capita land use has remained constant or very nearly so for thousands of years, with clearance thus linked to population in a nearly linear way. As a result, most land-use models have simulated very little pre-industrial clearance.

Recent work by Kaplan et al. (2009) showed that the assumption of constant land use is flawed. Historical land-use data paired with census counts show that much of Europe was deforested well before population began its steepest rise. This evidence requires that earlier farmers cleared far more land per-capita than predicted by the constant land-use assumption.

Ruddiman and Ellis (2009) noted seminal work by Boserup (1965, 1981) who proposed that a large and ongoing decrease in per-capita land use occurred during the Holocene. Farmers changed from shifting cultivation, which uses large amounts of land, to far more intensive agriculture based on annual or multiple crops per year. By some estimates, per-capita land use decreased by an order of magnitude through the last 7000 years.

The trend of decreasing land use in one region in southern China shown by Ellis and Wang (1997) in Figure 7B is further confirmed by the summary of Chao (1986) based on compilations by Buck (1937). This synthesis spans both the rice-growing areas in the south of China and the dry land crops in the north. Per-capita land use fell almost linearly by a factor of about four between AD 5 and the early–middle 1800s as farmers gradually learned to produce more food per hectare of land (Figure 8B). This factor of four decrease in per-capita land use has a linear trend similar to that estimated by Ruddiman and Ellis (2009) for the same interval, but average values were lower because Chao (1986) omitted other land uses and non-arable land in China.

Kaplan et al. (2011, this issue) applied the land-use pattern defined from European historical evidence to other regions, with an adjustment for higher productivity and lower per-capita land use in tropical regions with longer growing seasons. They found that China and India were largely deforested by 2000–1000 years ago and that early clearance was substantial in Peru, Mexico, and Sahelian Africa. They estimated a net pre-industrial release of 340 GtC, equivalent to a 24-ppm effect on atmospheric CO_2. This study suggests that small early farming populations released surprisingly large amounts of CO_2 to the atmosphere long before the industrial era.

The second major criticism of the early anthropogenic hypothesis is based on constraints imposed by the carbon isotopic composition of carbon dioxide ($\delta^{13}CO_2$). During the middle and late Holocene, atmospheric $\delta^{13}CO_2$ values varied within a narrow range around −6.35‰. This value reflects a balance between two carbon sources and sinks (Table 4). Terrestrial vegetation (mostly forests and peat) releases or stores organic carbon with an average $\delta^{13}C$ value near −25‰, whereas exchanges of inorganic carbon between the atmosphere and the ocean at −6‰ have no significant isotopic impact on atmospheric $\delta^{13}CO_2$.

Elsig et al. (2009) found a small average decrease of −0.05‰, with an even smaller decrease for the cracking method and a larger decrease for the sublimation method. Scaled to previous results from the Bern model (e.g. Joos et al., 2004), the ~−0.05‰ $\delta^{13}CO_2$ trend limits net emissions of −25‰ terrestrial carbon to ~50 GtC (Table 5).

Because of the small size of this total terrestrial contribution, Elsig et al. (2009) concluded that most of the observed 22-ppm Holocene CO_2 increase resulted from emissions of inorganic carbon from the ocean: ~10 ppm from carbonate compensation and ~5 ppm from coral-reef buildup. They relied on a model-based estimate of anthropogenic emissions from Strassman et al. (2008) of 50 GtC, equivalent to a CO_2 increase of ~3.5 ppm (Table 5). They also noted that 'some peat accumulation' (an estimated 40 GtC) occurred in boreal regions during the late Holocene, but they assumed that carbon storage in peat deposits was almost entirely offset by carbon released from regions like Africa where monsoons were weakening.
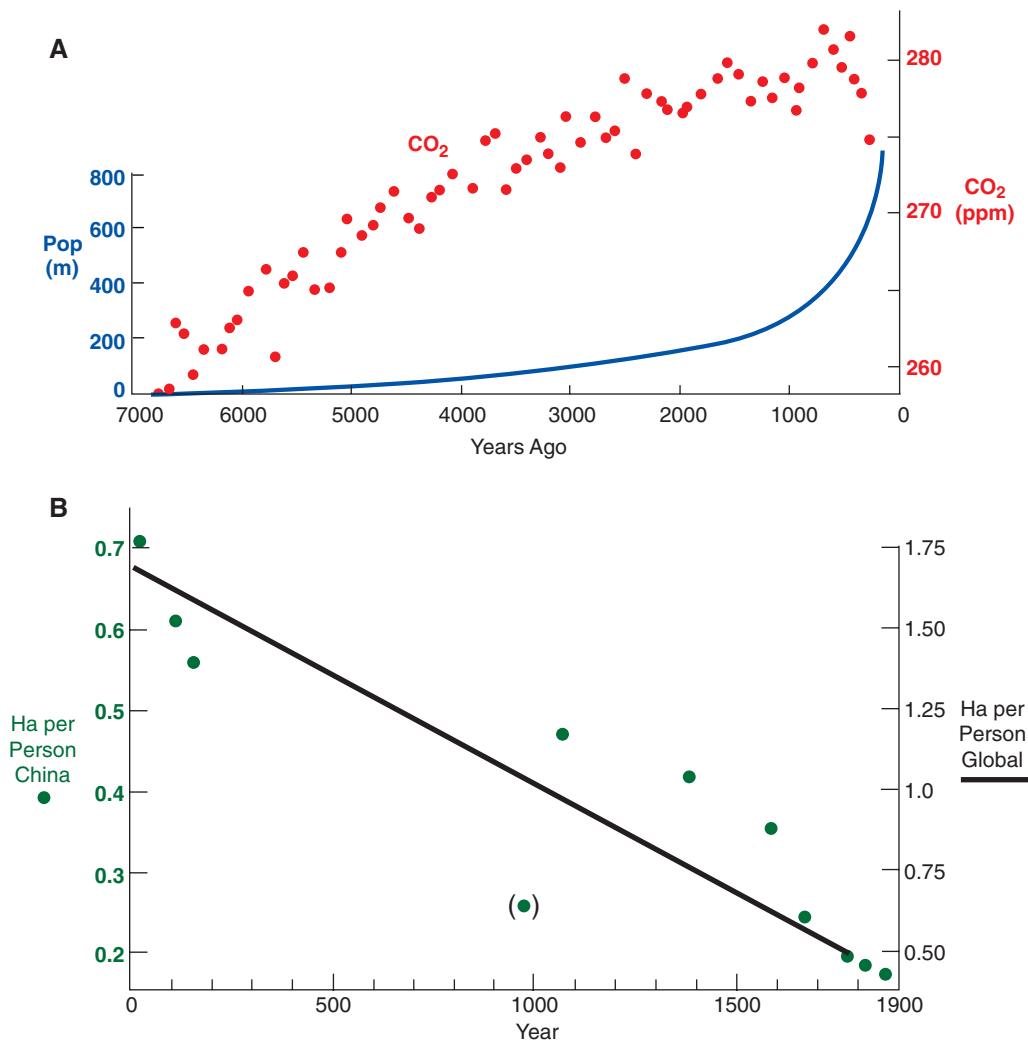
Figure 8. (A) Comparison of late Holocene CO_2 trend at Dome C (Luthi et al., 2009) with estimated global population (from Ruddiman and Ellis, 2009; based on Denevan, 1992 and McEvedy and Jones, 1978). (B) Per-capita land cultivation from Chinese historical records (Chao, 1986; based on Buck, 1937) compared with proposed late-Holocene trend of global per-capita land clearance from Ruddiman and Ellis (2009)

Table 5. Pre-industrial terrestrial carbon exchanges since ~7000 years ago

	Terrestrial carbon stored or released	
	Elsig et al. (2009)	This paper
Peat	**40 Gt stored**[a] (**~300 Gt @ −25‰**)	**275–280 Gt stored @ −27‰**[b]
Other natural terrestrial biomass	**30 Gt released**[c]	**20 Gt released**[d]
Anthropogenic	**50 Gt released**[e]	_[f]
$\delta^{13}CO_2$ trend	**50 Gt net release**[g]	**50 Gt net release**[g]
Residual	–	**330 Gt release**[h]

[a] Described in Elsig et al. as 'implied' (apparently an inferred residual value).
[b] From Yu (2011, this issue); see also Gorham (1991) and Gajewski et al. (2001).
[c] Taken from Indermuhle at al. (1999).
[d] Average of eight climate-model simulations: Foley (1994), Indermuhle et al. (1999), Francois et al. (1999), Brovkin et al. (2002), Kaplan et al. 2002), Joos et al. (2004), Wang et al. (2005), and Kleinen et al. (2010).
[e] Taken from Strassman et al. (2008); equivalent to a CO_2 increase of 3.5 ppm.
[f] Solved for as a residual (see below).
[g] Based on −0.05‰ trend since 7000 years ago.
[h] Anthropogenic contribution; equivalent to a CO_2 increase of 23 ppm. Derived as the residual of the peat storage, other terrestrial exchanges, and $\delta^{13}CO_2$ constraint, as shown above.

This analysis by the Bern group substantially underestimates the amount of carbon buried in boreal peat during the Holocene. Their 40 GtC value for the last 7000 years falls below the range of estimates from existing studies, and well below well-respected estimates. Gorham (1991) compiled evidence from ^{14}C-dated cores that indicated ~450 Gt of carbon burial since 13 000 years ago, of which ~300 GtC was buried in the last 6000 years (Gajewski et al., 2001).

Yu et al. (2009; Yu, 2011, this issue) have now assembled data from cores that span most of the boreal peat land regions and have multiple ^{14}C dates and bulk density data. Their analysis indicates that more than 270 GtC has been buried in boreal peat lands in the last 7000 years. They also estimated additional burial of a few GtC in tropical and Patagonian peat deposits during the last 7000 years, for a total combined carbon burial of 275–280 Gt (Table 5). Because peat carbon has a $\delta^{13}C$ value of −27‰, while other terrestrial carbon averages −25‰, we convert the 275–280 Gt of −27‰ peat carbon to ~300 Gt of −25‰ peat carbon for the purpose of the following mass-balance comparison in units of −25‰ terrestrial carbon.

The other major source/sink of terrestrial carbon is non-peat biomass: trees, shrubs, grass, litter, and upper soil layers (humus). Coupled climate/vegetation models have simulated changes

during the last 7000–6000 years that vary from a net release of ~100 GtC to a net storage of ~90 GtC (Table 5). This range of estimates reflects differing simulations of the major carbon sources (shrinking boreal and northern monsoon vegetation) and sinks (expanding monsoon vegetation in southern Amazonia, as well as increasing CO_2 fertilization as CO_2 values rose). Averaging these eight estimates gives a net release of ~20 GtC from the combined effects of natural processes, which reduces the net storage of −25‰ terrestrial carbon from 300 GtC to 280 GtC (Table 5).

The other constraint on the terrestrial carbon budget is the ~50 GtC release of terrestrial carbon indicated by the −0.05‰ $\delta^{13}CO_2$ trend during the last 7000 years (Elsig et al., 2009). The difference between this 50 GtC net release and the net storage of 280 Gt calculated above is 330 GtC – the net amount of terrestrial carbon not accounted for by all natural exchanges.

Anthropogenic deforestation appears to be the only viable explanation for this imbalance. This 330 GtC value is much larger than model simulations of pre-industrial emissions based on constant per-capita land use, but very close to the ~340 GtC of deforestation simulated by Kaplan et al. (2011, this issue). If fully equilibrated with the deep ocean, the 330 GtC of estimated deforestation emissions would be equivalent to a CO_2 effect of 23 ppm (Table 5).

The difference between the interpretation of Elsig et al (2009) and the one proposed here is somewhat analogous to an iceberg. Like the visible emergent tip of the ice (~10% of its total volume), the small size of the negative $\delta^{13}CO_2$ trend during the last 7000 years would seem to limit the amount of total (and anthropogenic) deforestation to a very small amount (Broecker and Stocker, 2006; Elsig et al, 2009; Joos et al., 2004). But hidden below the waterline is a very large mass of 'ice' – the much larger amount of anthropogenic deforestation required to balance the huge carbon storage in peat.

This estimated pre-industrial deforestation of ~330 GtC is larger than some previous estimates of total global Holocene CO_2 emissions from forest removal (for example, DeFries et al., 1999, based on Mathews, 1983 and on Leeman and Cramer, 1991). However, Olsen et al. (1983) noted that modern vegetation is a degraded (carbon-poor) version of true natural vegetation because humans have disturbed most remaining forested areas. In addition, modern climatologies underestimate natural carbon levels because of anthropogenic complications like reduced evapotranspiration in deforested monsoonal regions. After adjusting for these effects, Olsen et al. (1983) suggested that total carbon emissions could have been as large as 360 GtC.

Two related questions remain about the anthropogenic explanation of the late Holocene CO_2 trend (Table 6). (1) What is the total contribution from anthropogenic sources? (2) Can anthropogenic sources explain the $\delta^{13}C$ composition of the 22-ppm CO_2 increase?

Total pre-industrial emissions of terrestrial carbon from deforestation are estimated at 23–24 ppm based on the land-use simulation of Kaplan et al. (2011, this issue) and the revised $\delta^{13}CO_2$ mass-balance calculation (Tables 5, 6). In addition, as pointed out by Ruddiman (2007), direct anthropogenic CO_2 emissions are likely to have been supplemented by feedbacks from an ocean gradually warmed by rising CO_2 and CH_4 concentrations in the atmosphere. One feedback results from the temperature/solubility relationship. The ~0.2‰ trend toward lighter values during the last 7000 years in the marine $\delta^{18}O$ stack of Lisiecki and Raymo (2005) and the ocean–atmosphere modeling results from

Table 6. Anthropogenic contributions to late Holocene CO_2 increase

CO_2 source	Total effect on CO_2	Net effect on $\delta^{13}CO_2$ trend
Deforestation	23–24 ppm[a]	5 ppm[b]
Ocean CO_2 solubility feedback	9 ppm[c]	9 ppm[c]
Southern Ocean CO_2 feedback	? ppm[d]	? ppm[d]

[a]Based on Kaplan et al. (2011, this issue) and mass-balance calculation in Table 5.
[b]Based on constraint imposed by −0.05‰ change in $\delta^{13}CO_2$ since 7000 years ago (Elsig et al., 2009), converted to equivalent CO_2 change based on scaling from Joos et al. (2004).
[c]Based on benthic foraminiferal $\delta^{18}O$ trend in Lisiecki and Raymo (2004) and dynamic ocean model simulation in Kutzbach et al. (2011, this issue).
[d]Future simulation with an A/OGCM with ocean biogeochemistry will be required to estimate this. CO_2 feedback of 8 ppm from the Southern Ocean would explain the full 22-ppm CO_2 increase with the mean $\delta^{13}C$ composition measured by Elsig et al. (2009) and would also meet the full 40-ppm CO_2 anomaly proposed by Ruddiman (2003).

Kutzbach et al. (2011, this issue) both suggest a deep-ocean warming of ~0.8 to 0.9°C from this mechanism. Scaled to a 10-ppm change in atmospheric CO_2 per 1°C change in ocean temperature (Martin et al., 2005), this warming would have released enough CO_2 to support an atmospheric CO_2 increase of just under 9 ppm, bringing the anthropogenic total to ~32 pm (Table 6).

Although this estimate falls short of the 40-ppm CO_2 anomaly proposed by Ruddiman (2003), processes in the Southern Ocean are a second potential source of CO_2 feedback: changes in sea ice (Stephens and Keeling, 2000), in intensity and position of the westerlies (Toggweiler et al., 2006); and in upper-ocean stratification (Francois et al., 1997). If the Southern Ocean was warmer in the late Holocene than it would have been under a natural regime with greenhouse-gas decreases, CO_2 exchanges between the ocean and overlying atmosphere would have been higher, as would atmospheric CO_2 concentrations. In partial support of this idea, deuterium (δD) values at Dome C (Jouzel et al., 2007) fell early in all previous interglaciations, but remained nearly constant in the last 7000 years. Because δD values are tied to air temperature over Antarctica, these trends again indicate anomalous Holocene warmth.

In addition, model experiments reported by Kutzbach et al. (2009, 2011, this issue) simulated anomalous warmth over Antarctica that closely matched the amplitude of the late-Holocene δD anomaly at Dome C. The fact that the Antarctic region failed to cool as it had in previous interglaciations suggests that CO_2 levels in the atmosphere would have remained higher. It remains to be seen whether positive CO_2 feedback from the Southern Ocean (or from other responses in an anonymously warm ocean) can fill the remaining gap and meet the 40-ppm CO_2 anomaly originally hypothesized. Future A/OGCM experiments that include interactive ocean biochemistry will address this issue.

The second issue is the $\delta^{13}C$ composition of the 22-ppm CO_2 increase. The −0.05‰ $\delta^{13}CO_2$ trend from Elsig et al. (2009) limits the net terrestrial contribution during the last 7000 years to ~5 ppm (Table 6). As discussed earlier, this contribution primarily reflects a balance between a very large burial of carbon in peat deposits and an even larger anthropogenic release (Table 5). The remaining 17 ppm of the 22-ppm CO_2 increase must have come

from ocean sources. With 9 ppm explained by the temperature/solubility relationship, the remaining ~8 ppm would (again) have to come from the Southern Ocean (Table 6). In summary, deforestation emissions and ocean solubility feedback can satisfy ~80% (~32 out of 40 ppm) of the 40-ppm CO_2 anomaly originally proposed and can also account for >60% of the isotopic contributions to the $\delta^{13}CO_2$ trend. The role of the Southern Ocean remains a major unknown in these assessments.

Part 3. Conclusions

Science moves forward in part by falsification of competing hypotheses (Popper, 2002, based on work originally published in the 1930s and 1950s). Convincing falsification requires a very high standard of 'disproof' that can survive subsequent challenges.

A wide range of evidence on methane emissions meets this high standard and falsifies natural explanations for the late Holocene CH_4 increase. Downward methane trends during all seven previous interglaciations (Figure 2, Table 2) show that the upward trends in the late Holocene were anomalous and therefore highly unlikely to have been natural in origin. In addition, late-Holocene CH_4 emissions were falling in the two largest natural sources of methane on the planet (north tropical and boreal wetlands) and thus acting in opposition to the observed CH_4 increase. Although methane emissions from a third wetland source – the southern Amazon Basin – were rising, modeling studies show that these emissions are likely to have been considerably weaker and thus unlikely to have countered the larger decreases occurring in the north. An anthropogenic origin for the CH_4 increase is supported by Fuller et al. (2011, this issue), who synthesized archeological data that indicate large and exponentially rising methane emissions from rice irrigation in Asia between 5000 and 1000 years ago and additional (as-yet unquantified) emissions from the spread of livestock across Asia and Africa after 5000 years ago.

The debate over the origin of the late-Holocene CO_2 increase is not yet resolved, even though several papers from the Bern group previously claimed that the anthropogenic hypothesis can be rejected. Joos et al (2004) concluded 'The hypothesis by Ruddiman (2003) … is dismissed based on the ice core $\delta^{13}CO_2$ record and other well-founded land-use emissions estimates …'. Elsig et al. (2009) stated 'Our $\delta^{13}CO_2$ records render untenable suggestions that CO_2 emissions from anthropogenic land use changes caused the later Holocene CO_2 rise …'. Most recently, Stocker et al. (2010) noted 'Our results falsify the hypothesis that humans are responsible for the late Holocene CO_2 increase …;.

Several papers in this issue show that these claims of falsification were based on invalid evidence. One of two main arguments against the anthropogenic hypothesis was that early farming populations were too small to have emitted large amounts of CO_2, but this view has now been countered by evidence that early farmers used far more land per-capita than those in the centuries just before the industrial revolution (Figures 7, 8). Kaplan et al. (2011, this issue) reconstructed early clearance based on historical evidence of changing per-capita land use and found much greater early clearance and carbon emissions than land-use models based on constant per-capita land use over the last 7000 years. In addition, a new estimate of (anthropogenic) CO_2 feedback from the temperature–solubility relationship indicates a substantial pre-industrial contribution to the pre-industrial atmospheric CO_2 anomaly (Kutzbach et al., 2011, this issue).

A second argument for rejecting the early anthropogenic hypothesis has been the small amplitude of the negative $\delta^{13}CO_2$ trend during the last 7000 years. This constraint was thought to limit total emissions of terrestrial carbon to the atmosphere (including those from anthropogenic sources) to at most 5 ppm. In compiling their carbon-isotopic mass budget, however, Elsig et al. (2009) chose a value for late-Holocene carbon burial in boreal peat deposits of 40 Gt, which falls below most published estimates. A new estimate of just under 300 GtC from Yu (2011, this issue) is close to earlier estimates by Gorham (1991) and Gajewski et al. (2001). This much greater carbon burial in boreal peat over the last 7000 years, combined with model-based constraints on carbon exchanges from other natural processes, requires much larger anthropogenic emissions to balance the $\delta^{13}CO_2$ budget (Table 5).

A third argument for rejecting the early anthropogenic hypothesis has invoked a comparison of interglacial stages 11 and 1 that suggested that the current natural interglaciation still has 16 000 years left to run (Broecker and Stocker, 2006; EPICA, 2004). New evidence from stage 11 sea levels in the Red Sea (Rohling et al, 2010), along with closer inspection of the benthic $\delta^{18}O$ stack of Lisiecki and Raymo (2005), refutes this interpretation. The best-justified alignment of stages 11 and 1 indicates that the current interglaciation should have ended ~2000 years ago (or could end in the near future). In summary, the land-use, $\delta^{13}CO_2$ and stage 11 arguments that supposedly falsified the early anthropogenic hypothesis have all now been countered by new evidence that supports a strong early role by humans.

Two natural explanations for the CO_2 increase – delayed ocean carbonate compensation and coral reef construction – also remain viable, but both hypotheses face the problem that six of seven previous interglaciations fail to show any CO_2 increase. These prevalent mismatches suggest that the late-Holocene CO_2 increase is anomalous. The one interglaciation (stage 15) that shows a (small) CO_2 increase also has an anomalous benthic $\delta^{18}O$ trend that continued to decrease throughout the entire early-interglacial interval, instead of leveling out or beginning to increase as it did in the other interglaciations. This anomalous $\delta^{18}O$ trend suggests a no-analog situation early in stage 15 in which ongoing ice melting played a role in driving the CO_2 increase. All six other interglaciations fail to support natural explanations for the CO_2 increase.

Acknowledgments

References

Berger A (1978) Long-term variations of caloric insolation resulting from the Earth's orbital elements. *Quaternary Research* 9: 139–167.

Berger A and Loutre M-F (2003) Climate 400,000 years ago, a key to the future? *American Geophysical Union Geophysical Monograph* 137: 17–26.

Blunier T, Chappellaz J, Schwander J, Stauffer J and Raynaud D (1995) Variations in atmospheric methane concentrations during the Holocene epoch. *Nature* 374: 46–49.

Bird MI, Lloyd J and Farquhar GD (1996) Terrestrial carbon storage from the last glacial maximum to the present. *Chemosphere* 33: 1675–1685.

Boserup E (1965) The Conditions of Agricultural Growth. Allen and Unwin, 124 pp.

Boserup E (1981) *Population and Technological Change: A Study of Long Term Trends.* University of Chicago Press, 255 pp.

Broecker WS and Stocker TL (2006) The Holocene CO_2 rise: Anthropogenic or natural? *EOS Transactions American Geophysical Union* 87: 27.

Broecker WS, Clark E, McCorckle DC, Peng T-H, Hajdas I and Bonani G (1999) Evidence for a reduction in the carbonate ion content of the deep sea during the course of the Holocene. *Paleoceanography* 14: 744–752. doi:10.1029/1999PA900038.

Brook E and Mitchell L (2007) Timing and trends in Northern and Southern Hemisphere atmospheric Methane during the Holocene: New results from Antarctic and Greenlandic ice cores. Eos Transactions American Geophysical Union 88, Fall Meeting Abstract U21F-06.

Brook EJ, Harder S, Severinghaus J, Steig EJ and Sucher CM (2000) On the origin and timing of rapid changes in atmospheric methane during the last glacial period. *Global Biogeochemical Cycles* 14: 559–572.

Brovkin V, Bendtsen J, Claussen M, Ganopolski A, Kubatski C, Petoukhov V et al. (2002) Carbon cycle, vegetation, and climate dynamics in the Holocene: Experiments with the CLIMBER-2 model. *Global Biogeochemical Cycles* 16: 1139, doi:10.1029/2001GB001662.

Buck JL (1937) *Land Utilization in China.* Shanghai: Commercial Press, 494 pp.

Burns SJ (2011) Speleothem records of changes in tropical hydrology over the Holocene and possible implications for atmospheric methane. *The Holocene* XX: XX–XX (this issue).

Carcaillet C, Almquist H, Asnong H, Bradshaw RHW, Carrion JS, Gaillard M-J et al. (2002) Holocene biomass burning and global dynamics of the carbon cycle. *Chemosphere* 49: 845–863.

Chao K (1986) *Man and Land in Chinese History: An Economic Analysis.* Stanford University Press, 268 pp.

Chappellaz J, Blunier T, Kints S, Dallenbach A, Barnola J-M, Schwander J et al. (1997) Changes in the atmospheric CH_4 gradient between Greenland and Antarctica during the Holocene. *Journal of Geophysical Research* 102 D: 15 987–15 997.

COHMAP Members (1988) Climatic changes of the last 18,000 years: Observations and model simulations. *Science* 241: 1043–1052.

Crucifix M and Berger AL (2006) How long will our interglacial be? *EOS Transactions* American Geophysical Union 87: 352.

Cruz FW, Burns SJ, Karmann I, Sharp WD, Vuille M, Cardoso AO et al. (2005) Insolation-driven changes in atmospheric circulation over the past 116,000 years in subtropical Brazil. *Nature* 434: 64–66.

DeFries RS, Field CB, Fung I, Collatz GJ and Bounana L (1999) Combining satellite data and biogeochemical models to estimate global effects of human-induced land cover change on carbon emissions and primary productivity. *Global Biogeochemical Cycles* 13: 803–815.

Denevan WM (ed.) (1992) *The Native Population of the Americas in 1492.* University Wisconsin Press, 353 pp.

Ellis EC and Wang SM (1997) Sustainable traditional agriculture in the Tai Lake region of China. *Agriculture Ecosystems and Environment* 61: 177–193.

Elsig J, Schmitt J, Leuenberger D, Schneider R, Eyer M, Leuenberger F et al. (2009) Stable isotope constraints on Holocene carbon cycle changes from an Antarctic ice core. *Nature* 461: doi:10.1038/nature.08393

Emiliani C (1966) Paleotemperature analysis of Caribbean cores P6304-8 and P6304-9 and a generalized temperature curve for the past 425,000 years. *Journal of Geology* 74: 109–126.

EPICA Community Members (2004) Eight glacial cycles from an Antarctic ice core. *Nature* 429: 623–628.

Ferretti DF, Miller JB, White JWC, Etheridge DM, Lassey KR, Lowe DC et al. (2005) Unexpected changes to the global methane budget over the last 2,000 years. *Science* 309: 1714–1717.

Foley JA (1994) The sensitivity of the terrestrial biosphere to climate change: A simulation of the middle Holocene. *Global Biogeochemical Cycles* 8: 505–525.

Foley JA, Kutzbach JE, Coe MT and Levis S (1994) Feedbacks between climate and boreal forests during the Holocene epoch. *Nature* 371: 52–54.

Francois LM, Godderis Y, Warnant P, Rammstein G, de Noblet N and Lorenz S (1999) Carbon stocks and isotope budgets of the terrestrial biosphere at mid-Holocene and last glacial maximum times. *Chemical Geology* 159: 163–189.

Francois R, Altabet M, Yu E-F, Sigman D, Bacon MP, Frank M et al. (1997) Contribution of Southern Ocean surface-water stratification to low atmospheric CO_2 concentrations during the last glacial period. *Nature* 389: 929–935.

Fuller DQ, van Etten J, Manning K and Castillo C (2011) The contribution of rice agriculture and livestock pastoralism to prehistoric methane levels: An archaeological assessment. *The Holocene* XX: XX–XX (this issue).

Gajewski K, Viau A, Sawada M, Atkinson D and Wilson S (2001) Sphagnum peatland distribution in North America and Eurasia during the past 21,000 years*. Global Biogeochemical Cycles* 15: 297–310.

Gorham E (1991) Northern peatlands: Role in the carbon cycle and probable responses to climatic warming. *Ecological Applications* 1: 182–195.

Indermuhle A, Stocker T, Joos F, Fischer H, Smith HJ, Wahlen M et al. (1999) Holocene carbon-cycle dynamics based on CO_2 trapped in ice at Taylor Dome, Antarctica. *Nature* 398: 121–126.

Joos F, Gerber S, Prentice IC, Otto-Bleisner BL and Valdes P (2004) Transient simulations of Holocene atmospheric carbon dioxide and terrestrial carbon since the last glacial maximum. *Global Biogeochemical Cycles* 18: GB2002 10.1029/2003GB002156.

Jouzel J, Masson-Delmotte V, Cattani O, Dreyfus G, Falourd S, Hoffman G et al. (2007) Orbital and millennial Antarctic climate variability over the past 800,000 years. *Science* 317: 793–796.

Kaplan JO, Krumhardt KM and Zimmerman N (2009) The prehistoric and preindustrial deforestation of Europe. *Quaternary Science Reviews* 28: doi:10.1016/j.quascirev.2009.09.028.

Kaplan JO, Krumhardt KM, Ellis EC, Ruddiman WR, Lemmen C and Klein Goldwijk K (2011) Holocene carbon emissions as a result of anthropogenic land-cover change. *The Holocene* XX: XX–XX (this issue).

Kleinen T, Brovkin V, von Bloh W, Archer D and Munhoven G (2010) Holocene carbon cycle dynamics. *Geophysical Research Letters* 37: L02705. doi:10-1029/2009GL041391.

Kutzbach JE (1981) Monsoon climate of the early Holocene: Climate experiment with Earth's orbital parameters for 9000 years ago. *Science* 214: 59–61.

Kutzbach JE, Liu X, Liu Z and Chen G (2008) Simulation of the evolutionary response of global summer monsoons to orbital forcing over the last 280,000 years. *Climate Dynamics* 30: doi10:1007/s00382-007-0308-z.

Kutzbach JE, Ruddiman WF, Vavrus SJ and Phillippon G (2009) Climate model simulation of anthropogenic influence on greenhouse-induced climate change (early agriculture to modern). *Climatic Change* 99: doi:10.1007/s10584-009-9684-1.

Kutzbach JE, Vavrus SJ, Ruddiman WF and Philippon-Berthier G (2011) Comparisons of coupled atmosphere–ocean simulations of greenhouse gas-induced climate change for pre-industrial and hypothetical 'no-anthropogenic' radiative forcing, relative to present day. *The Holocene* XX: XX–XX (this issue).

Leeman R and Cramer WP (1991) *The IIASA Climate Data Base for Land Areas on a Grid with 0.5° Resolution.* Research report rr-91-18., Tech. Rep., International Institute for Applied System Analysis.

Lisiecki LE and Raymo ME (2005) A Plio-Pleistocene stack of 57 globally distributed benthic $\delta^{18}O$ records. *Paleoceanography* 20: PA1003, doi:10.1029/2004PA001071.

Loulergue L, Schilt A, Spahni R, Masson-Delmotte V, Blunier T, Lemieux B et al. (2008) Orbital and millennial-scale features of atmospheric CH_4 over the past 800,000 years. *Nature* 453: 383–386, doi.10.1038/nature06950.

Lüthi D, Le Flock M, Bereiter B, Blunier T, Barnola J-M, Siegenthaler U et al. (2008) High-resolution carbon dioxide concentration record 650,000–800,000 years before present. *Nature* 453: 379–382, doi:10.1038/nature06949.

Martin P, Archer D and Lea DW (2005) Role of deep sea temperatures in the carbon cycle during the last glacial. *Paleoceanography* 20: PA2015, doi: 10.1029/2003PA000914.

Mathews E (1983) Global vegetation and land use: New high resolution databases for climate studies. *Journal Climatology Applied Meteorology* 22: 474–487.

McEvedy C and Jones R (1978) *Atlas of World Population History*. Penguin, 368 pp.

Milankovitch MM (1941) *Canon of Insolation and the Ice-Age Problem*. Koniglich Serbische Akademie, Beograd, English translation by the Israel program for Scientific Translations, U.S. Deparment of Commerce, and National Science Foundation, Washington, DC.

Mischler JA, Sowers TA, Alley RB, Battle M, McConnell JR, Mitchell L et al. (2009) Carbon and hydrogen isotopic composition of methane over the last 1000 years. *Global Biogoechemical Cycles* 23: GB4024, doi:10.1029/2009GBC003460.

Olsen JS, Watts JA and Allison J (1983) *Carbon in Live Vegetation of Major World Ecosystems.* TN 37830 DOE/NBB Rep. TR004. Oak Ridge TN: Oak Ridge National Laboratory, 152 pp.,

Parrenin F, Barnola J-M, Beer J, Blunier T, Castellano E, Chapellaz J et al. (2007) The EDC3 chronology for the EPICA Dome C ice core. *Climate of the Past* 3: 485–497.

Popper KR (2002) *The Logic of Scientific Discovery*. (2nd edition) London: Routledge.

Ridgwell AJ, Watson AJ, Maslin MA and Kaplan JO (2003) Implications of coral reef buildup for the controls on atmospheric CO_2 since the Last Glacial Maximum. *Paleoceanography* 18: doi:10.1029/2003PA000893.

Rohling EJ, Braun K, Grant K, Kucera MM, Roberts AP, Siddall M et al. (2010) Comparison between Holocene and marine isotope stage 11 sea level histories. *Earth and Planetary Science Letters* doi:10.1016/j.epsl.2009.12.054.

Ruddiman WF (2003) The anthropogenic greenhouse era began thousands of years ago. *Climatic Change* 61: 261–293.

Ruddiman WF (2006) Comment on Broecker WS and Stocker TL The Holocene CO_2 rise: Anthropogenic or natural? *EOS Transactions American Geophysical Union* 87: 352–353.

Ruddiman WF (2007) The early anthropogenic hypothesis: Challenges and responses. *Reviews Geophysics* 45: RG4001 doi:10.1029/2006RG000207.

Ruddiman WF and Ellis EC (2009) Effect of per-capita land-use changes on Holocene forest clearance and CO_2 emissions. *Quaternary Science Reviews* 28: doi:10.1016/j.quascirev.2009.05.022.

Ruddiman WF and Raymo ME (2003) A methane-based time scale for Vostok ice. *Quaternary Science Reviews* 22: 141–153.

Ruddiman WF and Thomson JS (2001) The case for human causes of increased atmospheric CH_4 over the last 5000 years. *Quaternary Science Reviews* 20: 1769–1777.

Ruddiman WF, Guo Z, Zhou X, Wu H and Yu Y (2008) Early rice farming and anomalous methane trends. *Quaternary Science Reviews* 27: 1291–1295, doi:10.1016.jquascirev.2008.03.007.

Schmidt GA, Shindell DT and Harder S (2004) A note on the relationship between ice core methane and insolation. *Geophysical Research Letters* 31: L23206 doi:10.1029/2004GRL021083.

Selzer G, Rodbell D and Burns SJ (2000) Isotopic evidence for late glacial and Holocene hydrologic changes in tropical and South America. *Geology* 28: 35–38.

Stephens BB and Keeling RF (2000) The influence of Antarctic sea ice on glacial/interglacial CO_2 variations. *Nature* 404: 171–174.

Stocker B, Strassman K and Joos F (2010) Sensitivity of Holocene atmospheric CO_2 and the modern carbon budget to early human land use: Analyses with a process-based model. *Biogeosciences Discussions* 7: 921–952.

Strassman KM, Joos F and Fischer G (2008) Simulating effects of land use changes on carbon fluxes: Past contributions to atmospheric CO_2 increases and future commitments due to losses of terrestrial sink capacity. *Tellus* 60: 583–603. doi: 10.1111.j.1600-0889.2008.00340.x.

Toggweiler JR, Russell JL and Carlson SR (2006) Midlatitude westerlies, atmospheric CO_2, and climate change during the ice ages. *Paleoceanography* 21: 10.1029/2005PA001154.

Vecsei A and Berger WH (2004) Increase of atmospheric CO2 during deglaciation: Constraints on the coral reef hypothesis from patterns of deposition. *Global Biogeochemical Cycles* 18: GB1035. doi:10.1029/2003GB002147.

Wang Y, Mysack LA and Roulet N (2005) Holocene climate and carbon cycles dynamics: Experiments with the 'green' McGill paleoclimate model. *Global Biogeochemical Cycles* 19: GB3022. doi:10.1029/2005GB002484.

Wang Y, Cheng H, Edwards RL, He Y, Kong X, An Z et al. (2007) The Holocene Asian monsoon: Links to solar changes and North Atlantic climate. *Science* 308: 854–857.

Yu Z (2011) Holocene carbon flux histories of the world's peatlands: Global carbon-cycle implications. *The Holocene* XX: XX–XX (this issue).

Yu Z, Beilman DW and Jones MC (2009) Sensitivity of northern peatland carbon dynamics to Holocene climate change. *American Geophysical Union Geophysical Monograph Series* 10.1029/2008GM000822.

Zimov NS, Zimov SA, Zimova AE, Zimova GM, Chuprynin VI and Chapin FS III (2009) Carbon storage in permafrost and soils of the mammoth tundra-steppe biome. *Geophysical Research Letters* 36: L02502, doi:10.1029/2008GL036332.